International Journal on Emerging Technologies 10(2b): 73-78(2019)

ISSN No. (Print): 0975-8364
ISSN No. (Online): 2249-3255

Evaluation of Stress - Strain Relation on Rotational Motion of a Rotating Disc

Nishi Gupta, Shubham Goyal and Harjot Kaur
Department of Mathematics, Chandigarh University, Gharuan, Mohali, Punjab 140413, India.

(Corresponding author: Nishi Gupta)
(Received 02 May 2019, Revised 10 July 2019, Accepted 08 August 2019)
(Published by Research Trend, Website: www.researchtrend.net)

ABSTRACT: The effect of change due to angular speed on stable state creep behaviour of a rotating functional graded aluminium silicon carbide particle disc is examined by using Sherby's law. The stress and strain is obtained by taking pressure, volume and temperature constant with varying angular speed. It is investigated that the increase in the angular speed results in the increase of stress as well as strain in the rotating disc at two different angular speed of the disc.

Keywords: Composite, functionally graded material, rotational motion, creep, Sherby's law.

I. INTRODUCTION

Rotating discs have various engineering assumptions such as steam and gas turbine rotors, high speed gear engine, turbo generators, interior start engines, turbojet motors, responding and centrifugal compressors just to specify several. These applications perform components in conditions of effective services, life and power transportation are based on material speed of rotating and also working conditions other assumptions such as in aerospace engineering in which the various factors such as weight and durability at elevated temperature environment are so vital [27]. They have used FGM as special material. FGM are the combinations ceramic and metal. The ceramic materials provide elevated temperature resistance because of its low thermal conductivity. On different side the ductile metal prevent fracture caused by stress because of elevated temperature gradient in short time period. Steady -state strain rates in a rotating disk can be proscribed by choosing most favourable particle content and size of reinforcement. The thickness and density, stresses and strains in an elastic perfectly plastic isotropic revolving disk of consistent thickness and density by von Mises yield criteria [10]. Wahl *et. al.,* [1] calculated secondary creep deformation in revolving disk by von Mises and Tresca yield criteria theoretically as well as experimentally. He has concluded that the creep deformations calculated using von Mises criteria are too low in comparison to experimental results, which may be due to the anisotropy of the material used. Ma (1959) the shear stress theory is used to study the solid disc in a metallic gas at constant gas elevated temperature. The analysis is extended for gas turbine and jet engine disc to determine to the stress distributions over middle part of disk having variable thickness are moderately unique in relation to those apparent in a disc of consistent thickness. The exponential creep law is used to describe Secondary creep. Pandey *et al.* (1992) [5] analyzed the affect of volume fraction and size of reinforcement on the balanced state deformation behaviour of Al-SiC_p composites with temperature ranging 623 to 723k. The observation resulted that the stress exponents are more than 15 and empty activation is 294 KJ/mol. It was observed that the stress strain rate behaviour of composite arranged with stress dependent sub structure in variant model.

Jahed and Dubey (1997) [6] analysed primary, secondary deformation in axis symmetric problem in case of rotating disks and pressure vessels have been done. The technique uses the basic solution for a rotating uniform isotropic disc and generates the solution for non-uniform inhomogeneous one. Primary creep and secondary creep behaviour have been studied using anticipated method. Gupta *et al*. (2000) [7] examined that creep stresses rates and strain rates in a disk of variable thickness and density using Seth's transition theory. The result was obtained that the disk with density and thickness proportion diminishes is on more secure side as compare to flat disc having variable density. Singh *et al.,* [10] considered the effect of presence of residual stress on the rotating disc by using Norton's power law while comparing it with strain rate in disc without residual stress. You *et al.,* (2007) [13] implemented a simple method based on axis symmetric plane strain and steady state creep to determine stress and strain on functional graded material (FGM) of cylindrical vessels which were subjected to internal pressure. Singh *et al*., [16] performed creep analysis on an isotropic 6061 Al-20vol% SiC_w disc at the speed of 15000 rpm at temperature 561k by using Nortan's power law. Chen *et al.,* [17] experimented the coefficient of thermal expansion and aggregated plastic strain of pure Al-Matrix made of 50% silicon carbide particles within temperature 298 to 573k these disc contain SiC particle in matrix of pure aluminium. Rattan *et al.,* [18] explored the stable state deformation reaction of an isotropic functional graded material rotating disk of aluminium silicon carbide particle composites exposed to molecule inclination utilizing Sherby's law and inferred that the drag conduct in the disk can be constrained by the appropriate circulation of molecule substance as the strain rates are least when molecule substance is dispersed illustratively along the radial distance of disk.

Thakur *et al.,* (2013-2016) [21] observed the problem of rotating disk with thermal effect and heat generation due to variable thickness by using Seth's transition theory. Gupta *et al.,* (2016) [23] discussed the variant of Poisson ratios and thermal creep stresses also strain rates in an isotropic disc.

Thakur *et al.,* (2017) [27] examined the influence of thermal gradient on the stable state creep of the disk for three different cases. First case is the set at the uniform temperature of 625k while in the second case the temperature is 52k at inner radii and outer radii as 658k and 588k in the third case the disc operates at 110 k.

Singh *et al.,* (2018) [28] compared selective properties of composite material they examine Al-SiC have been best material, having high dissolving element, over the top thermal and electric conductivity and erosion resistance. Al-SiC have over the top tensile, right exhaustion, break habitations, high dissolving element, extreme flexibility, electric conductivity and great erosion resistance. Steel have malleable, over the top capacity to weight proportion due to this that has unnecessary vitality in saving through unit mass, metal gadgets may be small and light weight, never again like different building substances, steel can be impacts manufactured and generation colossally, bendy, sensibly estimated however steel is an alloy of iron. Silicon carbide (SiC) has high hardness, high thermal stability, low thermal increment, electric conductivity. SiC has many advantage utilized for high voltage, high temperature utility. The main aim of this paper is to evaluate the values of stress and strain in the rotating disk at various angular velocities.

II. ESTIMATION OF CREEP PARAMETERS

The balanced state creep reaction of the aluminum silicon carbide particle composite of changeable composition is depicted as far as of Sherby threshold stress based model given by

$$\dot{\varepsilon} = [M(\bar{\sigma} - \sigma_0)]^8$$

where, $$M = \frac{1}{E}\left[\frac{AD_L\lambda^3}{|\vec{b}_r|^5}\right]^{1/8} \tag{1}$$

where, $\bar{\sigma}$ is effective stress, "M" is material creep constant, D_L is the lattice diffusivity, λ is the sub grain size, A is the constant, $|\vec{b}_r|$ is the magnitude of Burger's vector, E is the young's modulus, σ_0 is the threshold stress.

After obtaining, values of creep parameters "M" and σ_0

These have been fit in the regression equation in the function of particle size, volume % and temperature. It has been determined that P = 1.7 μm , V = 10% and T = 623 k.

$$\ln M = (-34.91 + 0.2112 \ln P + 4.89 \ln T - 0.59 \ln V) \tag{2}$$

$$\sigma_0 = (-0.03507P + 0.01057T + 1.00536V - 2.11916) \tag{3}$$

III. MATHEMATICAL FORMULATION

-Consider a disk of aluminium silicon carbide (Al-SiC) of constant width having inner radii a, outer radii b revolving at angular speed and the applications are

Secondary condition of stress is supposed.

- Elastic deformations being relatively little for disk and may be ignored as compared to the creep deformation.
- The thickness is small as compared to its diameter therefore they assumed that axial stress is zero on the faces of disk.

-For biaxial state of stress, the globalized constitutive equations for deformation in an isotropic composite take the accompanying form when reference frame use along the principal directions *r* and *z.*

$$\dot{\varepsilon}_r = \frac{\dot{\bar{\varepsilon}}}{2\bar{\sigma}}\left[2\sigma_r - \sigma_\theta\right]$$

$$\dot{\varepsilon}_\theta = \frac{\dot{\bar{\varepsilon}}}{2\bar{\sigma}}\left[2\sigma_\theta - \sigma_r\right]$$

$$\dot{\varepsilon}_z = \frac{\dot{\bar{\varepsilon}}}{2\bar{\sigma}}\left[-(\sigma_r + \sigma_\theta)\right] \tag{4}$$

where, $\dot{\varepsilon}_r, \dot{\varepsilon}_\theta, \dot{\varepsilon}_z$ are strain rates and $\sigma_r, \sigma_\theta, \sigma_z$ stresses correspondingly in direction r, θ, z as indicate by subscripts.

Assuming that effective stress is based on mises criterion (1913, for biaxial state of stress, effective stress, $\bar{\sigma}$ is given as,

$$\bar{\sigma} = \frac{1}{\sqrt{2}}\left[\sigma_r^2 + \sigma_\theta^2 + (\sigma_r - \sigma_\theta)^2\right]^{1/2} \tag{5}$$

Using Eqns. (1) and (5) in consti. Eqn. (4), one gets,

$$\dot{\varepsilon}_r = \frac{d\dot{\mu}_r}{dr} = \frac{[M(\bar{\sigma} - \sigma_0)]^8(2x-1)}{2[x^2 - x + 1]^{1/2}} \tag{6}$$

$$\dot{\varepsilon}_\theta = \frac{\dot{\mu}_r}{r} = \frac{[M(\bar{\sigma} - \sigma_0)]^8(2-x)}{2[x^2 - x + 1]^{1/2}} \tag{7}$$

$$\dot{\varepsilon}_z = \frac{-[M(\bar{\sigma} - \sigma_0)]^8(x+1)}{2\left[(x)^2 - x + 1\right]^{1/2}} \tag{8}$$

where, x= σ_r / σ_θ is ratio of radial and tangential stress over any radii r. eqns.(6) and (7) can be calculated to attain σ_θ which is given by,

$$\sigma_\theta = \frac{(\dot{u}_a)^{1/8}}{M}\psi_1 + \psi_2 \tag{9}$$

where $$\dot{u}_a^{1/8} = \frac{\int_a^b M\sigma_\theta dr - \int_a^b M\psi_2 dr}{\int_a^b \psi_1 dr} \tag{10}$$

$$\psi_1 = \frac{\psi}{\left[x^2 - x + 1\right]^{1/2}} \tag{11}$$

$$\psi_2 = \frac{\sigma_0}{\left[x^2 - x + 1\right]^{1/2}} \tag{12}$$

$$\psi = \left[\frac{2\left[x^2 - x + 1\right]^{1/2}}{r(2-x)}\exp\int_a^r \frac{\phi}{r}dr\right]^{\frac{1}{8}} \tag{13}$$

and

$$\phi = \frac{(2x-1)}{(2-x)} \tag{14}$$

The stability of forces in radial direction are

$$\frac{d}{dr}\left[r\sigma_r\right] - \sigma_\theta + \rho\omega^2 r^2 = 0 \tag{15}$$

Int. Eqn. (15) from r = a to r = b and also putting the boundary condition $\sigma_r = 0$ at r = a and boundary condition $\sigma_r = 0$ at r = b one gets,

$$\int_a^b \sigma_\theta dr = \rho\omega^2(b^3 - a^3)/3 \tag{16}$$

In the first iteration, $\sigma_\theta = \sigma_{\theta_{avg}}$, where $\sigma_{\theta_{avg}}$ is average tang. Stress over cross segment of disk. Therefore (10) in first iteration is

$$\dot{u}_a^{1/8} = \frac{\sigma_{\theta_{avg}}\int_a^b M dr - \int_a^b M\psi_2 dr}{\int_a^b \psi_1 dr} \tag{17}$$

The values of σ_r can be obtained

$$\sigma_r = \frac{1}{r}\int_a^r \sigma_\theta \; dr \; - \frac{\rho\omega^2(r^3 - a^3)}{3r} \qquad (18)$$

Finding the values of σ_θ from Eqn. (9) radial stress σ_r is found by Eqn.(18) any point in composite disk also strain rate $\dot{\varepsilon}_r$ and strain rate $\dot{\varepsilon}_\theta$ is calculate from the Eqns. (6), (7) resp.

IV. NUMERICAL RESULTS

The strain and stress distribution of rotating aluminium silicon carbide particle (Al-SiCp) disc rotating motion at 13000 rpm and 15000 rpm are evaluated from the above mathematical modelling.

Table 1: Represents numerical calculation of radial/tangential stress and strain at different rotational motion of a rotating disc.

Angular speed	Radii	Radial/tangential stress and strain
ω=13000	r=40	σ_r = 0.8072 * 10^{15}
		σ_θ = 4.7398 * 10^{15}
		$\dot{\varepsilon}_r$ = -3.4783 * 10^{98}
		$\dot{\varepsilon}_\theta$ = 9.0651 * 10^{98}
ω=15000	r=40	σ_r = 0.3455 * 10^{16}
		σ_θ = 1.8899 * 10^{16}
		$\dot{\varepsilon}_r$ =-23.2715 * 10^{103}
		$\dot{\varepsilon}_\theta$ = 66.66 * 10^{103}
ω=13000	r=60	σ_r = 1.7007 * 10^{15}
		σ_θ = 4.7396 * 10^{15}
		$\dot{\varepsilon}_r$ = -1.0165 * 10^{98}
		$\dot{\varepsilon}_\theta$ = 5.9248 * 10^{98}
ω=15000	r =60	σ_r = 0.8064 * 10^{16}
		σ_θ = 1.8898 * 10^{16}
		$\dot{\varepsilon}_r$ = -0.7160 * 10^{103}
		$\dot{\varepsilon}_\theta$ = 7.9435 * 10^{103}
ω=13000	r=80	σ_r = 1.8727 * 10^{15}
		σ_θ = 4.7391* 10^{15}
		$\dot{\varepsilon}_r$ =-0.7237 * 10^{98}
		$\dot{\varepsilon}_\theta$ = 5.5611 * 10^{98}
		σ_r = 0.9997 * 10^{16}
ω=15000	r=80	σ_θ = 1.8889 * 10^{16}
		$\dot{\varepsilon}_r$ = -1.1939 * 10^{103}
		$\dot{\varepsilon}_\theta$ = 3.1339 * 10^{103}
ω=13000	r=100	σ_r = 1.6719 * 10^{15}
		σ_θ = 4.7389 * 10^{15}
		$\dot{\varepsilon}_r$ = -1.0654 * 10^{98}
		$\dot{\varepsilon}_\theta$ = 5.9809 * 10^{98}
ω=15000	r=100	σ_r = 1.0748 * 10^{16}
		σ_θ = 1.8877 * 10^{16}
		$\dot{\varepsilon}_r$ =-0.2991 * 10^{103}
		$\dot{\varepsilon}_\theta$ =3.1177 * 10^{103}
ω=13000	r=120	σ_r = 1.2210 * 10^{15}
		σ_θ =4.7385 * 10^{15}
		$\dot{\varepsilon}_r$ =-2.0760 10^{98}
		$\dot{\varepsilon}_\theta$ =7.4707 10^{98}
ω=15000	r=120	σ_r =1.0826 * 10^{16}
		σ_θ =1.8876 * 10^{16}
		$\dot{\varepsilon}_r$ =-0.3180 * 10^{103}
		$\dot{\varepsilon}_\theta$ = 3.1171 * 10^{103}
ω=13000	r=140	σ_r =0.5732 * 10^{15}
		σ_θ =4.7384 * 10^{15}
		$\dot{\varepsilon}_r$ =-4.6098 * 10^{98}
		$\dot{\varepsilon}_\theta$ =11.4299 * 10^{98}
ω=15000	r=140	σ_r = 1.0449 * 10^{16}
		σ_θ = 1.8872 * 10^{16}
		$\dot{\varepsilon}_r$ = -0.2234 * 10^{103}
		$\dot{\varepsilon}_\theta$ = 3.0419 * 10^{103}

IV. DISCUSSION AND GRAPHICAL REPRESENTATION

Fig. 1 represents the radial stress plotted at the angular speed 13000 rpm. It is examined that the radial stress is elevated at middle of disk as compared inner radii and outer radii. In the given Fig. 2, the radial stress is concluded at the angular speed 15000 rpm, it is examined that at inner radii the radial stress is lower and with increase in the radius of disk the radial stress again starts decreases. In Fig. 3, examined that the tangential stress is elevated at inner radii by increases the radial distance then tangential stress will decreases. The tangential stress is plotted at the angular speed 13000 rpm. It has

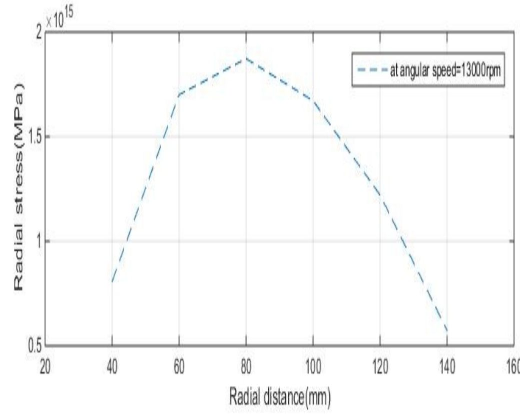

Fig. 1. Variation of radial stress along radial distance with Composite disk at the 13000 rpm

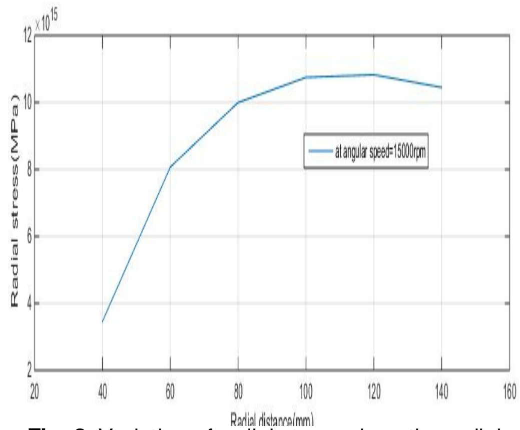

Fig. 2. Variation of radial stress along the radial distance with Composite disk at the 15000 rpm.

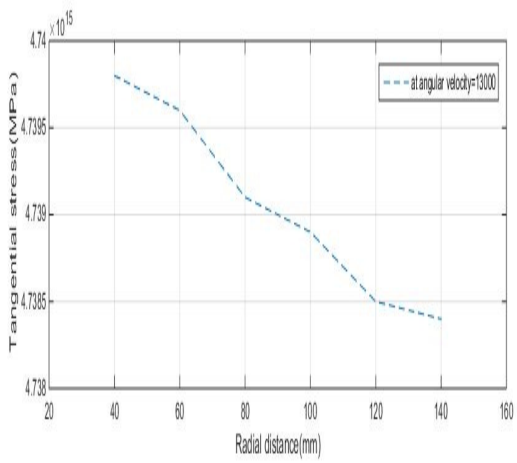

Fig. 3. Variation of tangential stress along radial distance with Composite disk at the 13000 rpm.

goes on raising but at the outer radii the radial stress

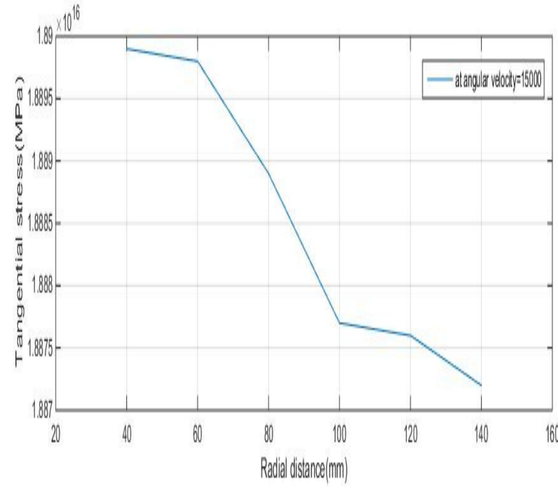

Fig. 4. Variation of tangential stress along radial distance with Composite disk at the 15000rpm.

In given Fig. 4, the tangential stress is plotted at the angular speed 15000 rpm. It is examined that the tangential stress is increases at inner radii and it starts decreases while increases the radius. In figure 5, the radial strain is concluded at the angular speed 13000 rpm. It is examined that the radial strain is elevated at the centre of the disk and lesser at the inner radius and outer radius. Also, outer radii are less radial strain than inner radii.

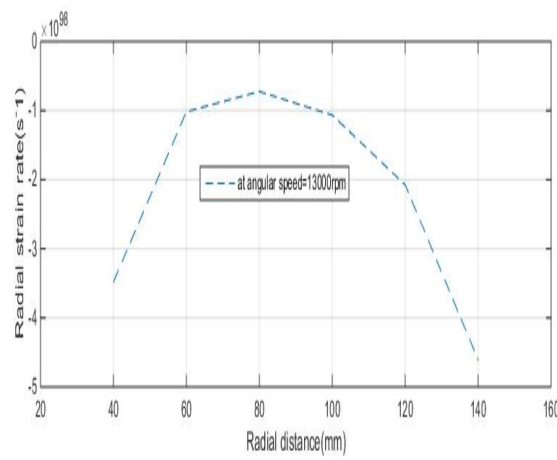

Fig. 5. Variation of radial strain along the radial distance with Composite disk at 13000 rpm.

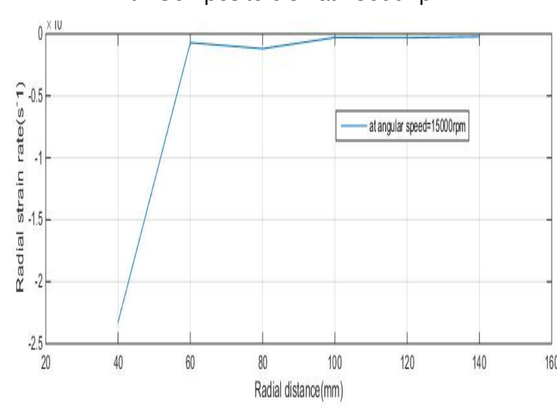

Fig. 6. Variation of radial strain along the radial distance with Composite disk at 15000 rpm.

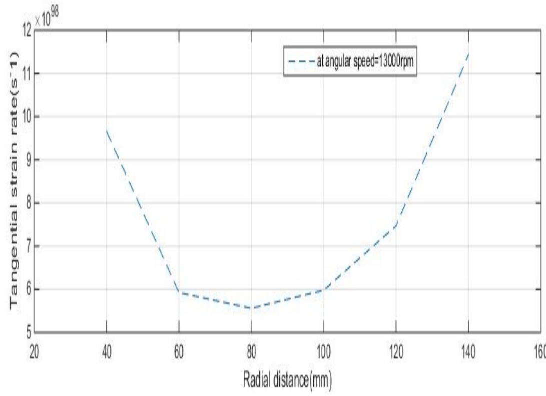

Fig. 7. Variation of tangential strain along radial distance with Composite disk at 13000 rpm.

In given Fig. 6, the radial strain is plotted at the angular speed 15000rpm it is examined that radial strain is lesser at the inner radii and it starts increases while we increase the radius and maximum at outer radius. In Fig. 7, the tangential strain is concluded at the angular speed 13000 rpm. It is examined that the tangential strain is higher at inner radii and outer radii of disk. The outer radii are more than inner radius and it is less at the middle of the disc. In Fig. 8, the tangential strain is concluded at the angular speed 15000rpm. It is examined that tangential strain is higher at inner radii and it starts decreases with the increase of radius and at the outer radii tangential stress is less. In the given Fig. 9, the radial stress along the radius at angular speed 13000/15000rpm is higher at centre of the disk. The radial stress higher for the disk rotating at 15000rpm as compared to the disk rotating at 13000rpm.

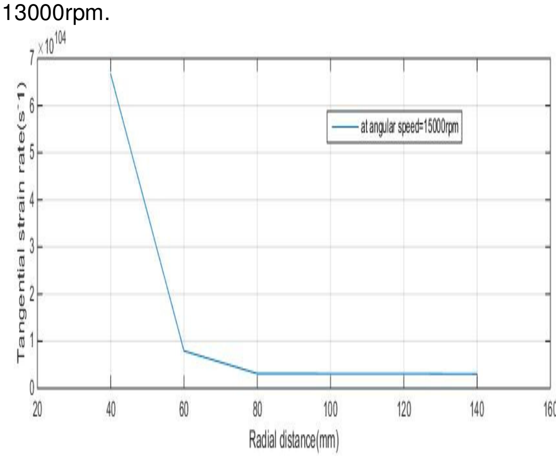

Fig. 8. Variation of tangential strain along radial distance with Composite disk at 15000 rpm.

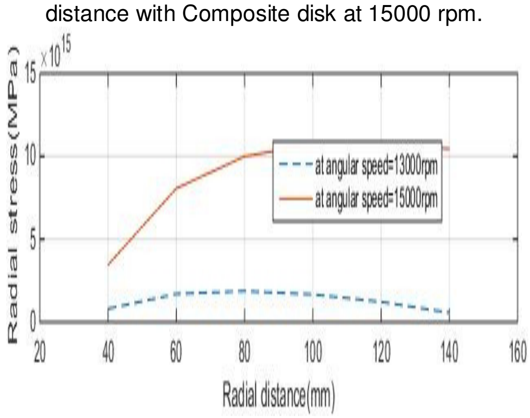

Fig. 9. Variation of radial stress along the radial distance with Composite disk at the 13000 rpm and 15000 rpm.

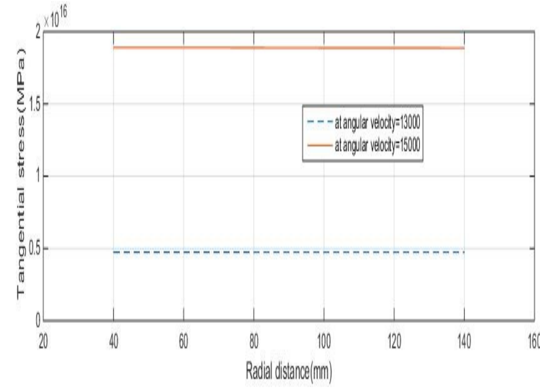

Fig. 10. Variation of tangential stress along radial distance with Composite disk at the 13000rpm and 15000 rpm.

In the given Fig. 10, tangential stress is represented along radius at angular speed 13000/15000 rpm. It is found that tangential stress at 15000 rpm is higher than angular speed of 13000 rpm. In this given Fig. 11, the radial strain is represented along radius at the angular speed 13000 rpm/15000 rpm. It is examined that the radial strain at the 13000rpm is higher than 15000 rpm at the inner radii and at the outer radii. In Fig. 12, the tangential strain is represented along radius at angular speed 13000/15000 rpm. It is found that tangential strain at the 15000 rpm is higher than 13000 rpm at the inner radii.

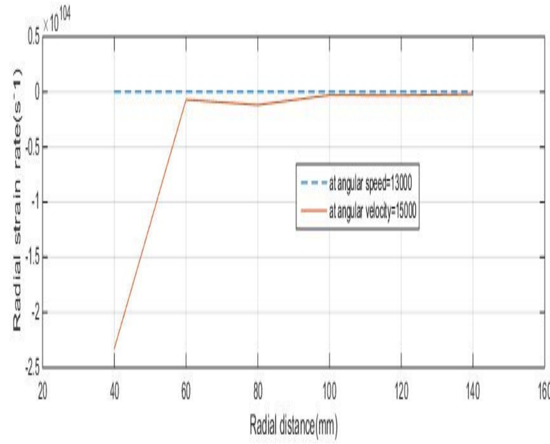

Fig. 11. Variation of radial strain along the radial distance with Composite disk at 13000 rpm and 15000 rpm.

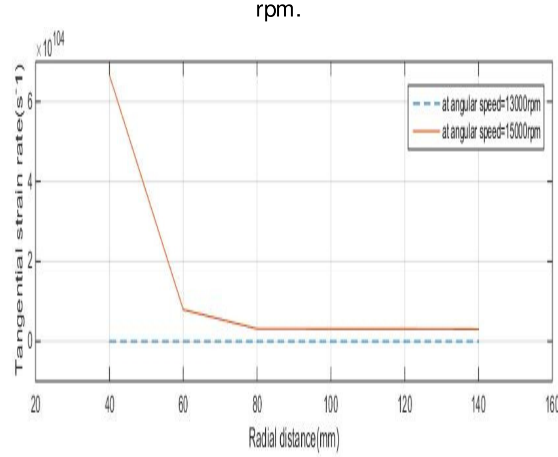

Fig. 12. Variation of tangential strain along the radial distance with Composite disk at the 13000 rpm and 15000 rpm.

V. CONCLUSIONS

It has been concluded that by increases in angular speed radial/tangential stress and strain is increased over entire radii in the isotropic disc operating at different angular speed. This analysis may be useful whenever one is interested in safe design of a rotating disk at high angular speeds

REFERENCES

[1]. Wahl, A. M., Sankey, G. O., Manjoine, M. J., & Shoemaker, E. (1954). Creep tests of rotating disks at elevated temperature and comparison with theory. *J. Appl. Mechanics*, **21**.

[2]. S. Bhatnagar, N., & P. Gupta, R. (1966). On the constitutive equations of the orthotropic theory of creep. *Journal of the Physical Society of Japan*, **21**(5), 1003-1007.

[3]. Bhatnagar, N.S., & Arya, V. K. (1974). Large strain creep analysis of thick-walled cylinders. *International Journal of Non-Linear Mechanics*, **9**(2), 127-140.

[4]. Arya, V.K., & Debnath, K. K. (1980). Creep analysis of orthotropic rotating cylinder. *Journal of Pressure Vessel Technology*, **102**, 371.

[5]. Pandey, A. B., Mishra, R. S., & Mahajan, Y. R. (1992). Steady state creep behaviour of silicon carbide particulate reinforced aluminium composites. *Acta Metallurgica et Materialia*, **40**(8), 2045-2052.

[6]. H Jahed , R Sethuraman & R. N. Dubey (1997). A variable material property approach for solving elastic-plastic problems. *International Journal of pressure vessels and piping,* **71**(3), 285-291.

[7]. Sing, S. B., Ray, S., Gupta, R. K., & Bhatnagar, N. S. (1998). Influence of anisotropy on creep in a whisker reinforced MMC rotating disc.

[8]. Singh, S. B., & Ray, S. (2001). Steady-state creep behaviour in an isotropic functionally graded material rotating disc of Al-SiC composite. *Metallurgical and Materials Transactions A*, **32**(7), 1679-1685.

[9]. Singh, S. B., & Ray, S. (2003). Newly proposed yield criterion for residual stress and steady state creep in an anisotropic composite rotating disc. *Journal of Materials Processing Technology*, **143**, 623-628.

[10]. Gupta, V. K., Singh, S. B., Chandrawat, H.N., & Ray, S. (2004). Steady state creep and material parameters in a rotating disc of Al–SiCP composite. *European Journal of Mechanics-A/Solids*, **23**(2), 335-344.

[11]. Alexandrova, N., & Alexandrov, S. (2004). Elastic–plastic stress distribution in a rotating annular disk. *Mechanics Based Design of Structures and Machines*, **32**(1), 1-15.

[12]. Pankaj, T. (2010). Elastic-plastic transition stresses in a thin rotating disc with rigid inclusion by infinitesimal deformation under steady state Temperature. *Thermal Science*, **14**(1), 209-219.

[13]. You, L. H., Ou, H., & Zheng, Z. Y. (2007). Creep deformations and stresses in thick-walled cylindrical vessels of functionally graded materials subjected to internal pressure. *Composite Structures*, **78**(2), 285-291.

[14]. Bayat, M., Saleem, M., Sahari, B. B., Hamouda, A. M. S., & Mahdi, E. (2008). Analysis of functionally graded rotating disks with variable thickness. *Mechanics Research Communications*, **35**(5), 283-309.

[15]. Sharma, S., & Sahni, M. (2008). Creep transition of transversely isotropic thick-walled rotating cylinder. *Adv. Theor. Appl. Mech*, **1**(7), 315-325.

[16]. Singh, S. B. (2008). One parameter model for creep in a whisker reinforced anisotropic rotating disc of Al–SiCw composite. *European Journal of Mechanics-A/Solids*, **27**(4), 680-690.

[17]. Chen, N., Zhang, H., Gu, M., & Jin, Y. (2009). Effect of thermal cycling on the expansion behavior of Al/SiCp composite. *Journal of materials processing technology*, **209**(3), 1471-1476.

[18]. Chamoli, N., Rattan, M., & Singh, S. B. (2010). Effect of anisotropy on the creep of a rotating disc of Al-SiCp composite. *International Journal of Contemporary Mathematical Sciences*, **5**(11), 509-516.

[19]. Rattan, M., Chamoli, N., & Singh, S. B. (2010). Creep analysis of an isotropic functionally graded rotating disc. *International Journal of Contemporary Mathematical Sciences*, **5**(9), 419-431.

[20]. Çallioğlu, H., Bektaş, N. B., & Sayer, M. (2011). Stress analysis of functionally graded rotating discs: analytical and numerical solutions. *ActaMechanica Sinica*, **27**(6), 950-955.

[21]. Pankaj, T., Singh, S. B., & Jatinder, K. (2013). Thickness variation parameter in a thin rotating disc by finite deformation. *FME Transactions*, **41**(2), 96-102.

[22]. Thakur, P., Singh, S. B., & LozanovićŠajić, J. (2015). Thermo elastic-plastic deformation in a solid disk with heat generation subjected to pressure. *Structure Integrity and Life*, **15**(3), 135-142.

[23]. Gupta, N., Satya, B. S., & Pankaj, T. (2016). Determine variation of poisson ratios and thermal creep stresses and strain rates in an isotropic disc. *Kragujevac Journal of Science*, **38**, 15-28.

[24]. Kaur, J., Thakur, P., & Singh, S. B. (2016). Steady thermal stresses in a thin rotating disc of finitesimal deformation with mechanical load.

[25]. Pankaj, T., Satya, B. S., Joginder, S., & Kumar, S. (2016). Steady thermal stresses in solid disk under heat generation subjected to variable density. *Kragujevac Journal of Science*, **38**, 5-14.

[26]. Thakur, P., Kaur, J., & Bir Singh, S. (2016). Thermal creep transition stresses and strain rates in a circular disc with shaft having variable density. *Engineering Computations*, **33**(3), 698-712.

[27]. Thakur, P., Gupta, N., & Satya, B. S. (2017). Thermal effect on the creep in a rotating disc by using Sherby's law. *Kragujevac Journal of Science*, **39**, 17-27.

[28]. Singh, S. Gupta, N. & Kaur, H. (2018). Systematic review on the study of material used in composite structure. *International Journal of Scientific & Engineering Research*, **9**:1559-1586.